Med Chem Res (2012) 21:663–671
DOI 10.1007/s00044-011-9576-6

MEDICINAL CHEMISTRY RESEARCH

ORIGINAL RESEARCH

Transition metal complexes of thiosemicarbazones with quinoxaline hub: an emphasis on antidiabetic property

Naveen V. Kulkarni · Vidyanand K. Revankar · B. N. Kirasur · Mallinath H. Hugar

Received: 5 May 2010 / Accepted: 17 January 2011 / Published online: 30 January 2011

Abstract New transition metal complexes of quinoxaline–thiosemicarbazone ligands were prepared and characterised by spectroanalytical techniques. The ligands L^1H_2 and L^2H_2 were obtained by the reaction of quinoxaline-2.3(1,4H)-dione with methyl and phenyl thiosemicarbazide, respectively. All the complexes are found to be monomeric in nature and have tetrahedral geometry. The copper complexes have shown redox responses in the applied voltage range, whereas the ligands and other complexes are electrochemically innocent. The ligands, copper and zinc complexes are explored for antidiabetic activity in the diabetes-induced Wister rats. Evaluation of antidiabetic activity was done by blood-glucose test and oral glucose tolerance test; few compounds have exhibited significant antidiabetic activity and posses low toxicity with a high safety profile.

Keywords Quinoxaline · Thiosemicarbazone · Antidiabetic agent · Blood-glucose test · Oral glucose tolerance test

N. V. Kulkarni · V. K. Revankar (✉)
Department of Studies in Chemistry, Karnatak University, Pavate Nagar, Dharwad 580 003, Karnataka, India
e-mail: vkrevankar@rediffmail.com

B. N. Kirasur
Basaveshwar Science College, Bagalkot 587 101, Karnataka, India

M. H. Hugar
Luqman College of Pharmacy, Gulbarga 585 102, Karnataka, India

Introduction

Diabetes Mellitus is a condition characterized by abnormal glucose levels with a tendency to hyperglycemia, due to a relative or absolute deficiency of insulin. It is caused by dysfunction of glucose homeostasis, afflicts over 140 million people worldwide and can lead to serious complications, such as retinopathy, nephropathy and neuropathy. Amongst them, insulin-dependent diabetes mellitus (IDDM) type 1, characterized by hyperglycemia due to absolute deficiency of insulin, requires the daily subcutaneous injections of insulin. On the other hand, non-insulin-dependent diabetes mellitus (NIDDM) type 2 can be treated with several drugs such as sulfonylureas, nateglinide, biguanides and pioglitazone etc. Though several types of therapeutics are developed for the treatment of type 2 diabetes, they have limited efficacy and tolerability and occasionally cause severe side effects (Moller, 2001).

In this regard, the approaches to synthesize better antidiabetic drugs are of immense interest. Quinoxaline derivatives have large applications in biochemistry and pharmacology as antimicrobial (Badran *et al*., 2003) antineoplastic agents and tumour-specific cytotoxins (Das *et al.*, 2009) and have exhibited significant in vitro activities against the human melanoma cell line A375, 110 (Deleuze-Masquefa *et al.*, 2009). Mayer and Taberner (2002) reported the utility of quinoxaline derivatives as blood glucose level reducing agents and insulinomimetic agent in mice. A series of 3-anilino-quinoxalinones has been identified as a new class of glycogen phosphorylase inhibitors by Dudash *et al.* (2005). They have made some incorporation to the quinoxaline scaffold with various aliphatic and aromatic compounds to produce novel analogues, some of which are 25 times more potent than the lead compound. Reddy Shastry *et al.* (1989) have prepared

the some *N*-arylcarbamoyl and arylthiocarbamoyl hydrazinoquinoxaline and evaluated their hyperglycemic activity in glucose primed rats. The compounds have shown a temperate order hypoglycemic activity (Reddy Shastry *et al*., 1989). These reports have explored antidiabetic strategy of quinoxalines and hence motivated researchers to synthesize various quinoxaline derivatives, which can serve as better antidiabetic agents for the future. Recently, Cu(II) and Zn(II) ions and their complexes have been found to exhibit in vitro insulinomimetic activity and in vivo antidiabetic (both type-1 and 2) effects in animals (Yasumatsu *et al*., 2007; Sakurai *et al.*, 2006). The complexation of these ions with ligands having antidiabetic molecules as backbone has been found to exhibit many fold enhancement in the activity (Yoshikawa *et al.*, 2005, 2009).

In this research study, quinoxaline-2,3-dione is selected as precursor and incorporated with thiosemicarbazide scaffolds to aid the coordinating and antidiabetic strategy. The synthesized SNO donor ligands are treated with Co(II), Ni(II), Cu(II) and Zn(II) ions to form the complexes and structural features of the compounds are explored. The ligands as well as Cu(II) and Zn(II) complexes are tested for the utility as antidiabetic drugs.

Experimental

Chemistry

Reagents and apparatus

Reagent grade chemicals were used for the preparation of precursors and purified solvents were used for the synthesis of ligands and complexes. Synthesis of quinoxaline 2,3-(1H,4H)-dione (Philips, 1928) and thiosemicarbazides (Sen and Gupta, 1962) was done according to the literature with slight modifications. The metal chlorides ($CoCl_2{\cdot}6H_2O$, $NiCl_2{\cdot}6H_2O$, $CuCl_2{\cdot}2H_2O$ and $ZnCl_2$) were used for the complex formation. C, H, N and S analysis was carried out on thermo quest elemental analyzer. Metal and chloride estimations were done by the standard procedures (Vogel, 1961). The molar conductivity measurements in DMF were made on ELICO-CM-82 conductivity bridge with conductivity cell having cell constant 0.51 cm^{-1}. The magnetic susceptibility measurements were made using Faraday balance at room temperature using $Hg[Co(SCN)_4]$ as calibrant. The ^1H NMR spectra were recorded in DMSO-d_6 solvent on Bruker-300 MHz spectrometer at room temperature using TMS as internal reference. IR spectra were recorded in KBr matrix using an Impact-410 Nicolet (USA) FT-IR spectrometer in 4000–400 cm^{-1} range. The electronic spectra of the complexes were recorded on a Hitachi 150-20 in the spectrophotometer in range 1000–200 nm. Cyclic voltammetric studies were performed at room temperature in DMF under oxygen free condition created by purging pure nitrogen gas, with CHI1110A Electrochemical analyzer (USA) comprising three electrode assembly of glassy carbon working electrode, platinum auxiliary electrode and Ag/AgCl reference electrode. Tetramethylammoniumchloride (0.01 M) was used as supporting electrolyte and instrument was standardized by ferrocene/ferrocenium redox couple. The ESR study of the copper complexes was carried out on a Varian E-4X-band EPR spectrometer, using TCNE as the g-marker. FAB mass spectra were recorded from JEOL SX 102/DA-6000 mass spectrometer using Argon/Xenon (6 kV, 10 mA) as the FAB gas and m-nitrobenzyl alcohol as matrix. TG and DTA measurements of the complexes were recorded in nitrogen atmosphere on Universal V2 4F TA instrument at the heating rate of 10°C/min and scan range of 25–800°C.

Chemistry

Synthesis

Synthesis of thiosemicarbazone ligands

0.1 M of thiosemicarbazide [(methyl thiosemicarbazide, 1.05 g) (phenyl thiosemicarbazide, 1.66 g)] in 100 ml methanol was treated with quinoxaline 2,3-(1,4H)-dione (1.62 g, 0.1 M). The reaction mixture was refluxed for 3–4 h and the dirty/greenish yellow solid separated was filtered, washed 2–3 times with ethanol and dried (Fig. 1).

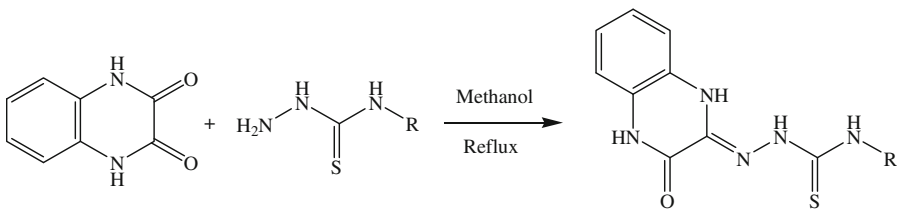

For L^1H_2, R = CH_3 and for L^2H_2, R= C_6H_5

Fig. 1 Schematic representation of preparation of ligands

[Note: The preparation of ligand L^2H_2 has been reported earlier with different synthetic route (Reddy Shastry *et al*., 1989)].

Synthesis of complexes

A methanolic solution (100 cm^3) of metal(II) chloride [$CoCl_2 \cdot 6H_2O$ (0.237 g, 0.01 M), $NiCl_2 \cdot 6H_2O$ (0.237 g, 0.01 M), $CuCl_2 \cdot 2H_2O$ (0.170 g, 0.01 M) and $ZnCl_2$ (0.135 g, 0.01 M)] was added with stirring to an ethanolic solution of the ligand [L^1H_2 (0.267 g, 0.01 M), L^2H_2 (0.329 g, 0.01 M)] and refluxed at water bath temperature for 3–4 h. So obtained solid complex was separated by filtration under suction, washed with hot ethanol and dried in vacuo.

Pharmacology

Animals for the investigation

Male Wister rats weighing about 180–200 g were used in this analysis with prior permission from institutional animal ethics committee (IAEC). Animal studies were performed as per the rules and regulations of CPCSEA. The animals were acclimatized to the experimental room having normal temperature (23 ± 2°C), controlled humidity conditions and 12:12 h light and dark cycle. The Wister rats were housed in sterile Plexiglas transparent cages containing sterile paddy husk as bedding material with maximum of four animals in each cage. The rats were fed on autoclaved standard rat food pellets and water ad libitum.

Acute toxicity test (Mishra et al., 1973)

During the administration of a chemical substance to the biological system, different types of interactions can occur and a series of dose-related responses result. In most cases these responses are desired and useful, but there are a number of other effects which are not advantageous. These may or may not be harmful to the biological system. Hence in the pharmacological evaluation of any synthesized or isolated compound, it is customary to carryout acute toxicity study to determine the safe effective dose of the novel compound. Acute toxicity is involved in estimation of LD_{50} (the dose which has proved to be lethal (causing death) to 50% of the tested group of animals).

Wister rats weighing between 180 and 200 g were starved for 18 h before the experiment. The animals were divided into the group of eight each, after recording their body weight. The test sample solutions of suitable concentration in 1% gum acacia were administered orally in different groups. Initially all test samples were administered with 12.5 mg/kg body weight, if all the animals survived with this dose, then the samples were tested at higher dose range viz., 25, 50, 100 and 200 mg/kg and if the test samples caused 100% death at this dose the lower dose range was treated as LD_{50} dose. Finally, the administered dose 150 mg/kg is fixed for all the compounds.

Alloxan-induced diabetes

Diabetes was induced by a single intra peritoneal injection of 150 mg/kg body weight of alloxan monohydrate (S.D. Fine Chem. Ltd., Mumbai.) in 0.9% NaCl saline (O Neil *et al*., 2001). After 72 h of alloxan injection, blood glucose was measured by glucometer. The diabetic rats (glucose level > 300 mg/dl) were separated and used for the study (Wright, 1951).

Glibenclamide (standard drug antidiabetic used in this study) in its pure form was obtained from Sun Pharmaceuticals Ltd., Andheri (East), Mumbai, India, made as an aqueous solution and was injected daily for 9 days (as a 600 μg/kg body weight) using an intra gastric tube (Breslin *et al*., 2003).

Methodology

The weighed animals were divided into nine groups of six animals each. Group 1 served as normal healthy control and received food (standard pellet rodent diet) and vehicle only. Group 2 served as diabetic control group. Group 3 served as standard control group and received glibenclamide (600 μg/kg body weight) in the form of aqueous suspension. The volume of suspension was 1 ml/100 gm body weight of rat. Groups 4–9 received the prepared compounds (150 mg/kg body weight). The different groups received the drug before the food by intragastric tube. In this study the doses (glibenclamide, ligands, copper and zinc complexes) were administered once a day for 9 days.

Collection of blood and estimation of blood glucose levels

At the end of the treatment period, two drops of blood was collected from rat tail vein after 16 h fasting. The pulsatum gluco-strips (stored in refrigerator) taken out from the sachet and glucometer is calibrated to 660 units according to the specification mentioned in the strips. The blood removed from the rat tail vein was immediately spread on the marked end of the strip. The strip was inserted in the glucometer and the blood glucose level, reading was recorded.

Oral glucose tolerance test (OGTT) (Nawrocka, 1996)

Animals were fasted for 12 h divided into nine groups of six rats each. Group 1 was served as normal healthy control and received food (standard pellet rodent diet) and vehicle only. Group 2 served as diabetic control group. Group 3 served as standard control group and received glibenclamide (600 μg/kg body weight) in the form of aqueous suspension. The volume of suspension was 1 ml/100 gm of rat. Groups 4–9 received ligands and their copper and zinc complexes (150 mg/kg body weight) as a fine tween-80 suspension. After 30 min, the rats of all groups were orally given with 400 mg/kg body weight of glucose. Blood samples were collected from the rat tail vein just before glucose administration and at 30, 60 and 90 min after glucose loading. Blood levels were measured immediately by using glucometer.

Statistical analysis

Values are expressed as mean ± SEM, statistical difference between means were determined by performing one-way ANOVA followed by Dunnett's test. $P < 0.05$ was considered as significant difference in this study.

Results and discussion

The transition metal complexes prepared in this course were non-hygroscopic (stable at the room temperature) and in the form of amorphous solids. These are soluble easily in DMSO, DMF and sparingly in ethanol and methanol, whereas they are insoluble in chlorinated hydrocarbons. The elemental analysis data of the ligands and their complexes along with molar conductivity values are compiled in Table 1.

Molar conductivity results

The molar conductance values of the complexes measured at room temperature in DMSO solution with 10^{-3} mol/dm^3 concentration fall in the range 14.3–18.7/ohm cm^2/mol indicating the non-electrolytic nature of the complexes (Geary, 1971). Comparatively high values are due to the solvation effect of DMSO, which replaces anion from the coordination sphere.

IR spectral studies

The important IR spectral bands of ligands and corresponding complexes along with assignments are presented in Table 2.

The absence of a band in the region 2500–2600 cm^{-1}, which is characteristic of thiol group [ν(C-SH)], suggest the stable thione form of the ligands and hence decline the thione–thiol tautomerism (H–N–C=S $\Leftrightarrow$ > C=N–SH) in the present set of thiosemicarbazone ligands. The thioamidic coupled vibrations, I [ν(CN) and ν(NH) + δ(CH)], II [ν(CN) and ν(CS)], III [ν(CS) and ν(CS) + ν(CN)] and IV[ν(CS)] are observed around 1600, 1545, 1460 and 940 cm^{-1} confirm the thioketo form of ligands (Kulkarni *et al*., 2010). The ν(C=O) of quinoxaline ring was observed as a sharp, intense band at ~1675 cm^{-1} and the stretching vibrations of azomethine functionality ν(C=N) were observed near 1645 cm^{-1}. The quinoxaline ring ν(NH) and hydrazine ν(^{2}NH) were observed around 3300 cm^{-1} as broad intense band.

In all the complexes, the band due to ν(C=O) has not observed due to the coordination of oxygen through enol mode. A new band appeared around 1260 cm^{-1} attributable to ν(C–O) confirms the same. But in the ^{1}H NMR studies no peak which can be assigned to –OH (enol form) is observed for the zinc complexes due the coordination of oxygen after deprotonation. The band due to ν(C=N) has

Table 1 Chemical composition and molar conductivity data of compounds

Compounds	Colour	Yield in percentage	Elemental analysis (%) calculated (found)					Molar conductance (mho cm^2/mol)
			C	H	N	S	M	
L^1H_2	Dirty yellow	82	48.19 (48.28)	4.41 (4.52)	28.12 (28.05)	12.83 (12.89)	–	–
$[CoL^1(H_2O)]$	Dark brown	80	38.21 (38.32)	3.50 (3.57)	22.29 (22.33)	10.19 (10.23)	18.63 (18.58)	12.1
$[NiL^1(H_2O)]$	Dark brown	82	38.27 (38.24)	3.50 (3.58)	22.32 (22.39)	10.20 (10.26)	18.66 (18.71)	14.2
$[CuL^1(H_2O)]$	Greenish black	81	37.68 (37.72)	3.44 (3.37)	21.94 (22.01)	10.03 (10.14)	19.90 (19.96)	13.2
$[ZnL^1(H_2O)]$	Yellow	79	37.38 (37.84)	3.42 (3.49)	21.80 921.75)	9.96 (10.03)	20.40 (20.32)	11.3
L^2H_2	Greenish yellow	83	58.06 (57.98)	3.87 (3.93)	22.58 (22.67)	10.82 (11.04)	–	–
$[CoL^2(H_2O)]$	Brown	84	46.51 (46.43)	3.10 (3.18)	18.08 (18.15)	8.26 (8.32)	15.21 (15.30)	13.2
$[NiL^2(H_2O)]$	Dark brown	80	46.57 (46.65)	3.10 (3.04)	18.11 (18.18)	8.27 (8.18)	15.13 (15.21)	12.7
$[CuL^2(H_2O)]$	Black	82	45.85 (45.96)	3.06 (3.14)	17.87 (17.95)	8.17 (8.26)	16.25 (16.37)	13.6
$[ZnL^2(H_2O)]$	Greenish yellow	83	45.74 (45.65)	3.04 (3.04)	17.78 (17.86)	8.13 (8.22)	16.64 (16.53)	13.5

Table 2 Infrared spectral data of ligands and complexes in cm^{-1}

Compounds	ν(OH) water	ν(N–H)	ν(C=O)	ν(C=N)	Thioamide bands				ν(C–O)	ν(C–S)	ν(M–N)	ν(M–S)
					I	II	III	IV				
L^1H_2	–	3350s	1674s	1644s	1599s	1540s	1460s	939m	–	–	–	–
$[CoL^1(H_2O)]$	3400b	3379b	–	1631s	1589s	1536s	1403w	–	1265	751s	611m	450m
$[NiL^1(H_2O)]$	3432b	3314b	–	1636s	1605s	1518m	1390m	–	1264	754s	629m	440m
$[CuL^1(H_2O)]$	3422b	3300b	–	1640m	1600s	1551s	1411m	–	1265	766s	599s	437m
$[ZnL^1(H_2O)]$	3445b	3300b	–	1636s	1598s	1546s	1411m	–	1263	753s	602m	413s
L^2H_2	–	3376b	1676s	1645s	1602s	1542s	1470s	944m	–	–	–	–
$[CoL^2(H_2O)]$	3419b	3376b	–	1640s	1599s	1540s	1410w	–	1268	753s	601m	430m
$[NiL^2(H_2O)]$	3418b	3300b	–	1641s	1601s	1546s	1433w	–	1267	753s	601m	406s
$[CuL^2(H_2O)]$	3407b	3288b	–	1652s	1605s	1517m	1430m	–	1264	759m	602m	420m
$[ZnL^2(H_2O)]$	3449b	3326b	–	1650m	1615s	1517m	1401s	–	1260	725m	617m	470s

s sharp; *m* medium; *b* broad; *w* weak

been shifted to the lower frequency side in all the complexes, owing to the coordination of azomethine nitrogen. The thioamide bands having major contribution from the ν(C=S) group (thioamide bands IV and III, respectively) have disappeared or experienced a fall in intensity and frequency upon complexation suggesting the thioenolisation and subsequent sulphur coordination. It is further supported by the strong signal at 760 cm^{-1} attributable to ν(C–S).

The absence of ν(S–H) in the complexes suggests the coordination of sulphur through deprotonation. The bands due to ν(NH) are broadened in all the complexes due to the overlapping of ν(OH) bands of coordinated water molecule. The low frequency non-ligand bands in the 600–625 cm^{-1} and 400–450 cm^{-1} region are assigned to ν(M–N) and ν(M–S), respectively.

^{1}H NMR studies

The ligand L^1H_2 displays two sharp singlets at 11.91 and 10.71 ppm attributed to the two ring NHs of quinoxaline core. The first signal was disappeared on complexation with Zn(II) ion, indicating the enolisation and subsequent coordination of oxygen via deprotonation. Whereas the second signal experiences a significant up field upon complexation. Hydrazine NH observed at 8.89 ppm in ligand has been disappeared on complexation due to the thioenolisation. No peak corresponding to –SH was observed in the spectrum indicating the sulphur coordination through deprotonation. Amine proton resonating at 7.98 ppm, shift to the low field region and the methyl protons experience a deshielding upon complexation and shift to 4.97 ppm. The aromatic protons observed in the region 7.24–6.92 ppm show small shifts in complex, due to variation in electron density and steric constraints brought about by chelation. Water coordination is evidenced by the broad peak at 3.70 ppm (Table 3).

In ligand L^2H_2, sharp singlets observed at 10.29, 9.81, 9.00 and 8.03 ppm are assigned to ring NHs, hydrazine NH and amine NH, respectively. Upon complexation peaks at 10.29 and 9.00 ppm were disappeared due to the coordination of oxygen and sulphur via deprotonation. Aromatic protons are distributed in the region 7.99–6.89 ppm and suffer a small variation in the resonance frequency upon complexation. The coordinated water resonates at 3.50 ppm as broad peak.

Electronic spectral studies

The intense peaks in the range 250–275 nm observed in both ligands are due to intra ligand π–π^* transitions. These bands remain almost unchanged in the spectra of complexes. The

Table 3 NMR spectral data

Compounds	^{1}H NMR δ (ppm)					
	Quinoxaline–NH	Hydrazine–NH	R–NH	Aromatic protons	$-CH_3$	Coordinated H_2O
L^1H_2	11.91 and 10.71	8.89	7.98	7.24–6.92	3.50	–
$[ZnL^1(H_2O)]$	8.19	–	7.51	7.44–7.10	4.97	3.70
L^2H_2	10.29 and 9.81	9.00	8.03	7.99–6.89	–	–
$[ZnL^2(H_2O)]$	9.84	–	8.09	7.95–6.95	–	3.50

ligands also show a broad band at 325 nm with a shoulder on low energy side, due to n–π^* transition associated with azomethine linkage (Lever, 1968). In complexes this band experiences bathochromic shift due to the coordination of azomethine nitrogen. The broad peak centred at 365 nm in the ligand is assigned to n-π^* of thioamide chromophore, it suffers blue shift in complexes due to thioenolisation (Naik *et al*., 2002a, b). The electronic spectra of the copper and nickel complexes are virtually identical. The band observed at 450 nm is assigned to S → M charge transfer (LMCT) transition ($\varepsilon \sim$ 20000/lcm/M) (Naik *et al*., 2002a, b). The *d–d* transitions are observed around 820 nm as low intensity hump ($\varepsilon \sim$ 100/lcm/M). Cobalt complexes exhibit asymmetric broad peak around 600–700 nm ($\varepsilon \sim$ 200/lcm/M) corresponding to the *d–d* transition (Bailar *et al*., 1975). The broad intense peak with high extinction coefficient observed around 420 nm is attributed to LMCT transition. The zinc complexes display the peaks around 400 nm attributed to LMCT along with the intra-ligand transitions.

Magnetic properties

The room temperature magnetic moment values of nickel and cobalt complexes were found to be 2.80, 2.81, 4.18 and 4.21 BM for [$NiL^1(H_2O)$], [$CoL^1(H_2O)$], [$NiL^2(H_2O)$] and [$CoL^1(H_2O)$], respectively, suggesting the four coordinated, tetrahedral geometry (Bailar *et al*., 1975; Dutta and Syamal, 1993). Whereas copper complexes [$CuL^1(H_2O)$] and [$CuL^2(H_2O)$] exhibit the magnetic moment values (μ_{eff}) 1.52 and 1.56 BM, respectively (Table 4). Fairly lower magnetic moment values of copper complexes are attributed to the higher covalancy of S–Cu bond and lower orbital contribution of sulphur (Kulkarni *et al*., 2010).

EPR spectral analysis

The copper complexes [$CuL^1(H_2O)$] and [$CuL^2(H_2O)$] exhibit isotropic intense broad signals with g_{iso} values 2.09 and 2.05, respectively, in the solid state X-band EPR spectral analysis. Broad EPR spectra of this kind were reported earlier for the complexes having large organic ligand substituents with different donor atoms having considerable covalent character for metal–ligand bonds (Kulkarni *et al*., 2010; Seleem *et al*., 2005).

FAB mass spectral analysis

The copper complexes of L^1H_2 and L^2H_2 exhibit intense peaks at *m*/*z* 319 and 392, respectively, which is in line with the molecular formula [$ML(H_2O)$] assigned for the complexes. Along with the molecular ion peak, spectra exhibit various other peaks with different intensity and *m*/*z* value, which are attributed to molecular cations of various fragments of complexes. The proposed structures of complexes are given in Fig. 2.

Thermal studies

To determine the thermal stability of complexes and their decomposition pattern TG and DTA studies were carried out. The complexes were analysed in the nitrogen atmosphere and the heating rate of 10°C/min is maintained.

The studies reveal that both the complexes [$CuL^1(H_2O)$] and [$CuL^2(H_2O)$] decompose in two steps. The first step of disintegration of [$CuL^1(H_2O)$] corresponds to the loss of one water molecule with reduction of ~5.72% total mass in the range 75–120°C, the corresponding differential peak (DTA) suggests the endothermic nature of the process. Second stage of mass loss of 14.76% at the range 250–380°C is ascribed to the ligand decomposition. The final product was found to be stable metal oxide, as suggested by the plateau region in the thermogram. [$CuL^2(H_2O)$] exhibits a similar pattern of thermal decomposition with 4.97% weight loss at the range 60–110°C representing the endothermic process of loss of one water molecule. The decomposition of 7.25 and 37.2% in the

Table 4 The electronic spectra and magnetic moment data

Compounds	λmax (nm)	μ_{eff} (B.M)
L^1H_2	260, 278, 325, 368	–
[$CoL^1(H_2O)$]	248, 336, 426, 620, 675	4.18
[$NiL^1(H_2O)$]	347, 371, 435, 480, 830	2.80
[$CuL^1(H_2O)$]	304, 369, 465, 826	1.52
[$ZnL^1(H_2O)$]	300, 338, 375, 422	Diamagnetic
L^2H_2	248, 275, 318, 358, 368	–
[$CoL^2(H_2O)$]	250, 348, 422, 630, 680	4.21
[$NiL^2(H_2O)$]	321, 352, 375, 420, 460, 824	2.81
[$CuL^2(H_2O)$]	311, 342, 363, 468, 825	1.56
[$ZnL^2(H_2O)$]	340, 372, 421	Diamagnetic

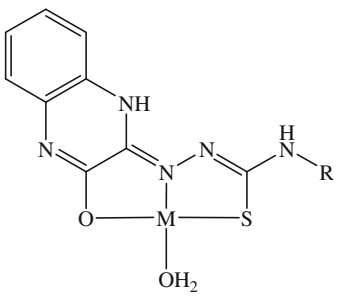

Where M = Co, Ni, Cu and Zn

For L^1H_2, R = CH_3 and for L^2H_2, R= C_6H_5

Fig. 2 Proposed structure of complexes

range 150–250 and 250–500°C, respectively, corresponds to the ligand disintegration. The plateau region at the higher temperature range indicates the stable metal oxide formation.

Cyclic voltammetry studies

The complexes, as a solution of DMSO were scanned in potential range of −1 to 1 V in nitrogen atmosphere. In this case of investigation, only the copper complexes exhibit redox behaviour in the applied potential range (Table 5). Both the ligands were found to be electrochemically innocent indicating that the redox behaviour of copper complexes is purely metal based. The other complexes of both series did not show any responses in the applied potential range. The typical cyclic voltammograms of $[CuL^1(H_2O)]$ and $[CuL^2(H_2O)]$ are shown in Fig. 3.

$[CuL^1(H_2O)]$ shows one oxidation peak at 0.49, 0.45 and 0.41 V with the varying scan rates of 0.15, 0.1 and 0.05 V/s, respectively, during the anodic potential scan and in the reverse scan (cathodic scan) it exhibits a reduction peak at −0.25, −0.20 and −0.13 V, respectively. Similarly $[CuL^2(H_2O)]$ also exhibits redox responses corresponding to the couple Cu(II)/Cu(III). It shows oxidation peak at 0.24, 0.20 and 0.17 V (for the scan rates 0.15, 0.1 and 0.05 V/s, respectively) and corresponding reduction peak at 0.04, −0.01 and −0.01 V, respectively.

The analysis reveals that both the copper complexes exhibit quasi reversible redox processes (the separation between cathodic and anodic peak potentials ($\Delta Ep = Epa - Epc$) for the redox couple Cu(II)/Cu(III) is greater than 60 mV, the value of peak potentials depends on scan rate and values of peak current ratio (Ipc/Ipa) are almost constant but not unity) (Naik *et al.*, 2002a, b).

Table 5 Cyclic voltammetry results

Complex	Scan rate (V/S)	*E*pa (V)	*E*pc (V)	Δ*E*p (V)[a]	$E_{1/2}$ (V)[b]	*I*pc/*I*pa
$[CuL^1(H_2O)]$	0.15	0.49	−0.25	0.74	0.12	0.78
	0.1	0.45	−0.20	0.65	0.125	0.82
	0.05	0.41	−0.13	0.54	0.14	0.88
$[CuL^2(H_2O)]$	0.15	0.24	0.04	0.20	0.14	0.82
	0.1	0.20	0.01	0.19	0.11	0.86
	0.05	0.17	−0.01	0.18	0.08	0.91

[a] $\Delta Ep = Epa - Epc$

[b] $E_{1/2} = [Epc + Epa]/2$

Acute toxicity study

In acute toxicity study all the tested compounds did not show significant toxic effects and found to be safe at the tested dose level of 1500 mg/kg body weight of Wister rat.

Blood glucose level test

The results of blood glucose level test are shown in Table 6. All the tested compounds have shown good activity in the reduction of blood glucose level as compared with the diabetic control rats. The complex $[ZnL^1(H_2O)]$ and ligand L^2H_2 have showed significant reduction in blood glucose level, as efficient as glibenclamide, a standard drug used.

OGTT

The results of OGTT are shown in Table 6. At the 30 min interval after the oral administration of glucose, the compounds $[ZnL^1(H_2O)]$ and $[CuL^2(H_2O)]$ have shown good activity and have reduced the blood glucose level notably as compared to the glibenclamide. At the 90 min interval, the compounds $[CuL^1(H_2O)]$, $[ZnL^1(H_2O)]$ and $[CuL^2(H_2O)]$ have shown significant reduction in blood glucose level.

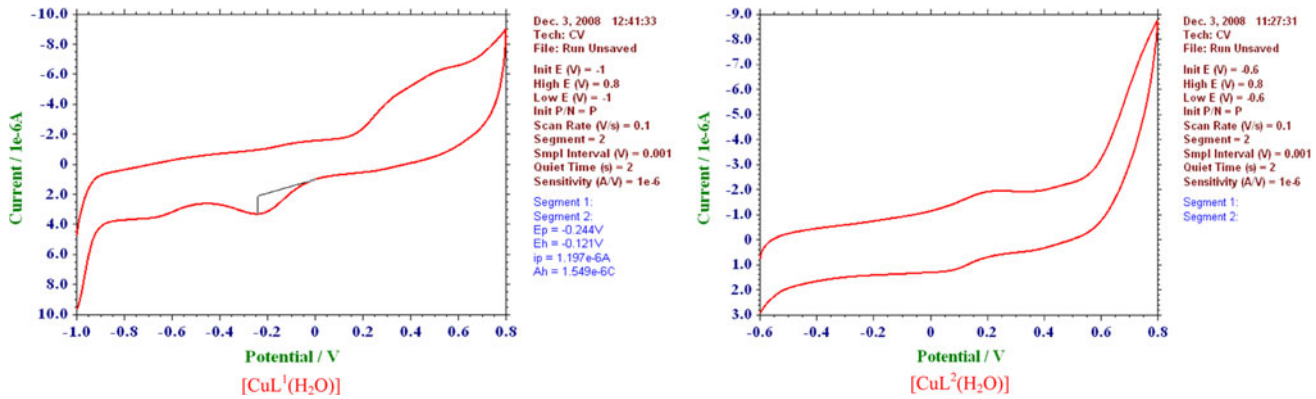

Fig. 3 Voltammograms of $[CuL^1(H_2O)]$ and $[CuL^2(H_2O)]$ at the scan rate 0.1 V/s

Table 6 Effect of ligands and complexes on blood glucose level of alloxan-induced diabetic Wister rats after prolonged treatment and OGTT in normal Wister rats

Treatment and groups	Blood glucose level in mg/dl		OGTT in non-diabetic rats		
	Basal	9th day	Fasting	30 min	90 min
Control (normal saline)	76.32 ± 1.42	78.22 ± 1.02	80.12 ± 1.60	188.12 ± 4.22	136.62 ± 2.80
Diabetic control (alloxan)	326.6 ± 3.20	342.42 ± 1.80	–	–	–
Glibenclamide (std drug)	332.3 ± 4.80	142.4 ± 2.60	79.80 ± 3.22	176.8 ± 3.02	102.8 ± 2.30***
L^1H_2	323.0 ± 6.82	332.0 ± 22.6	82.26 ± 2.58	180.8 ± 4.44	120.6 ± 2.33
$[CuL^1(H_2O)]$	324.7 ± 6.12	335.6 ± 12.30	76.17 ± 2.60	178.60 ± 3.42	110.8 ± 3.72***
$[ZnL^1(H_2O)]$	325.0 ± 7.68	188.8 ± 22.8**	76.22 ± 2.58	156.6 ± 2.20	106.3 ± 2.18***
L^2H_2	312.70 ± 8.2	182.2 ± 16.4**	72.40 ± 1.82	176.6 ± 2.32	122.8 ± 3.30
$[CuL^2(H_2O)]$	320.0 ± 7.58	318.04 ± 10.8	75.60 ± 2.58	156.60 ± 10.38	118.0 ± 2.44***
$[ZnL^2(H_2O)]$	356.0 ± 10.58	333.6 ± 18.2	80.53 ± 2.40	182.8 ± 3.09	124.70 ± 14.48

One-way ANOVA followed by Dunnet's '*t*' test. Values are expressed as mean ± SEM. $P > 0.05$ is considered as non-significant. $P < 0.05$ is considered as significant

** $P < 0.01$ as compared to diabetic control group

*** $P < 0.001$ as compared to diabetic control group

According to the earlier studies, drugs cause antidiabetic effect by promoting regeneration of β cells or by protecting the cells in pancreas from destruction, by restricting glucose load as well as by promoting unrestricted endogenous insulin action or they effect β cells to release insulin and activate the insulin receptors to absorb the blood sugar (e.g., sulphonylureas) (Fosset *et al.*, 1988). The comparable effect of prepared compounds with glibenclamide suggests the similar mode of action. Since alloxan permanently destroys the pancreatic β cells and the compounds have lowered the blood glucose level in alloxanised rats to significant level, indicating that the compounds possess extra pancreatic effects. The compounds showed beneficial effects on blood glucose and hyperlipidemia associated with diabetes, thus they could serve as good adjuvant to other oral hypoglycemic agents and seems to be promising for the development of medicines for diabetes mellitus. Further, detailed studies are necessary to find out the active constituents, which are responsible for the said activity and its exact mechanism of action.

Conclusion

All the complexes are found to be monomeric and tetrahedral in nature. Both the ligands act as SNO tridentate dibasic chelates and the coordinated water molecule satisfies the fourth place in tetra coordinated systems. The copper complexes undergo redox reaction in the applied range of potential (−1 to +1 V) and exhibit quasireversible responses. The ligands and their copper and zinc complexes are explored for antidiabetic activity in the diabetes-induced Wister rats. Evaluation of antidiabetic activity was done by blood-glucose test and OGTT. The compounds $[ZnL^1(H_2O)]$ and L^2H_2 have showed notable reduction in blood glucose level. The complexes $[CuL^1(H_2O)]$, $[ZnL^1(H_2O)]$ and $[CuL^2(H_2O)]$ have exhibited promising activity in OGTT and posses low toxicity with a high safety profile.

Acknowledgments The authors thank Department of Chemistry and USIC, Karnatak University, Dharwad for the spectral facility. Recording of FAB-mass spectra (CDRI Lucknow) are gratefully acknowledged. Further, the author (Naveen V. Kulkarni) thank Karnatak University, Dharwad for providing Nilekani fellowship.

References

Badran MM, Abouzid KAM, Hussein MHM (2003) Synthesis of certain substituted quinoxalines as antimicrobial agents (part II). Arch Pharm Res 26:107–113

Bailar JC, Emeleus HJ, Nyholm SR, Dickenson AFT (1975) Comprehensive inorganic chemistry. Pergamon Press, New York, p 3

Breslin HJ, Miskowski TA, Kukla MJ, De Winter HL, Somers MVF, Roevens PWM, Kavash RW (2003) Tripeptidyl-peptidase II (TPP II) inhibitory activity of (S)-2,3-dihydro-2-(1H-imidazol-2-yl)-1H-indoles, a systematic SAR evaluation. Part 2. Bioorg Med Chem Lett 13(24):4467–4471

Das U, Pati HN, Panda AK, De Clerc E, Balzarini J, Molnár J, Baráth Z, Ocsovszki I, Kawase M, Zhou L, Sakagami H, Dimmock JR (2009) 2-(3-Aryl-2-propenoyl)-3-methylquinoxaline-1,4-dioxides: a novel cluster of tumor-specific cytotoxins which reverse multidrug resistance. Bioorg Med Chem 17:3909–3915

Deleuze-Masquefa C, Moarbess G, Khier S, David N, Gayraud-Paniagua S, Bressolle F, Pinguet F, Bonnet PA (2009) New imidazo [1, 2-a]quinoxaline derivatives: synthesis and in vitro activity against human melanoma. Eur J Med Chem 44:3406–3411

Dudash J Jr, Zhang Y, Moore JB, Look R, Liang Y, Beavers MP, Conway BR, Rybczynski PJ, Demarest KT (2005) Synthesis and

evaluation of 3-anilino-quinoxalinones as glycogen phosphorylase inhibitors. Bioorg Med Chem Lett 15:4790–4793

Dutta RL, Syamal A (1993) Elements of magneto chemistry, 2nd edn. E. W. Press, New Delhi

Fosset M, De Weille JR, Green RD, Schmid-Antomarchi H, Lazdunski M (1988) Antidiabetic sulfonylureas control action potential properties in heart cells via high affinity receptors that are linked to ATP-dependent K+ channel. J Biol Chem 263: 7933–7936

Geary WJ (1971) The use of conductivity measurements in organic solvents for the characterisation of coordination compounds. Coord Chem Rev 7:81–122

Kulkarni NV, Hegde GS, Kurdekar GS, Budagumpi S, Sathisha MP, Revankar VK (2010) Spectroscopy, electrochemistry, and structure of 3D-transition metal complexes of thiosemicarbazones with quinoline core: evaluation of antimicrobial property. Spectrosc Lett 43:235–246

Lever ABP (1968) Inorganic electronic spectroscopy. Elsevier Publishing Company, New York

Mayer G, Taberner PV (2002) Effects of the imidazoline ligands (±)-efaroxan and KU14R on blood glucose homeostasis in the mouse. Eur J Pharmacol 454:95–102

Mishra AK, Dandiya PC, Kulkarni SK (1973) Anticonvulsant activity of some trimethoxybenzylidene-2-thiohydantoin derivatives. Indian J Pharmacol 5:449–450

Moller DE (2001) New drug targets for type 2 diabetes and the metabolic syndrome. Nature 414:821–827

Naik AD, Annigeri SM, Gnagadharmath UB, Revankar VK, Mahale VB, Reddy VK (2002a) Anchoring mercapto-triazoles on dicarbonyl backbone to assemble novel binucleating, acyclic SNONS compartmental ligands. Indian J Chem 41A:2046–2053

Naik AD, Annigeri SM, Gangadharmath UB, Revankar VK, Mahale VB (2002b) Bimetallic complexes of a potentially pentadentate, acyclic, symmetrical compartmental Schiff base ligand that provides suitable topology for an exogenous bridge. Trans Met Chem 27:333–336

Nawrocka W (1996) Syntheses and pharmacological properties of new 2-aminobenzimidazole derivatives. Boll Chi Farm 135: 18–23

O Neil MJ, Smith M, Heckelman PE (eds) (2001) The Merck Index, 13th ed, Merck & Co. Inc., New Jersey. Monograph Number, 10074, p 1785

Philips MA (1928) The formation of 2-substituted benziminazoles. J Chem Soc 2393–2399

Reddy Shastry CV, Marwah P, Shankar Rao G (1989) Synthesis and biological activity of some new *N*-aryl carbamoyl and aryl thiocarbamoyl hydrazinoquinoxalin-2-ones. Indian J Chem 28B: 885–891

Sakurai H, Katoh A, Yoshikawa Y (2006) Chemistry and biochemistry of insulin mimeticvanadium and zinc complexes, trial for treatment of diabetes mellitus. Bull Chem Soc Jpn 79:1645–1664

Seleem HS, Shetary BAEL, Khalil SME, Mostafa M, Shebl M (2005) Structural diversity in copper(II) complexes of bis(thiosemicarbazone) and bis(semicarbazone) ligands. J Coord Chem 58:479–493

Sen AB, Gupta SK (1962) Possible antiamoebic agents part XIX. Synthesis of 1,3,4-thiadiazolines and di-1, 3,4-thiadiazolines. J Ind Chem Soc 39:628–634

Vogel AI (1961) A text book of quantitative inorganic analysis, 3rd edn. Longmans Green and Co., Ltd, London, p 266

Wright JB (1951) The chemistry of the benzimidazoles. Chem Rev 48:397–537

Yasumatsu N, Yoshikawa Y, Adachi Y, Sakurai H (2007) Antidiabetic copper(II)-picolinate: impact of the first transition metal in the metallopicolinate complexes. Bioorg Med Chem 15: 4917–4922

Yoshikawa Y, Kondo M, Sakurai H, Kojima Y (2005) A family of insulinomimetic zinc(II) complexes of amino ligands with Zn(Nn) (n = 3 and 4) coordination modes. J Inorg Biochem 99:1497–1503

Yoshikawa Y, Hirata R, Yasui H, Sakurai H (2009) Alpha-glucosidase inhibitory effect of anti-diabetic metal ions and their complexes. Biochimie 91:1339–1341